GEOPHYSICS, VOL. 69, NO. 3 (MAY-JUNE 2004); P. 699–707, 15 FIGS.
10.1190/1.1759456

Quartic moveout coefficient for a dipping azimuthally anisotropic layer

Andrés Pech* and Ilya Tsvankin‡

ABSTRACT

Interpretation and inversion of azimuthally varying nonhyperbolic reflection moveout requires accounting for both velocity anisotropy and subsurface structure. Here, our previously derived exact expression for the quartic moveout coefficient A_4 is applied to P-wave reflections from a dipping interface overlaid by a medium of orthorhombic symmetry.

The weak-anisotropy approximaton for the coefficient A_4 in a homogeneous orthorhombic layer is controlled by the anellipticity parameters $\eta^{(1)}$, $\eta^{(2)}$, and $\eta^{(3)}$, which are responsible for time processing of P-wave data. If the dip plane of the reflector coincides with the vertical symmetry plane $[x_1, x_3]$, A_4 on the dip line is proportional to the in-plane anellipticity parameter $\eta^{(2)}$ and always changes sign for a dip of 30°. The quartic coefficient on the strike line is a function of all three η–parameters, but for mild dips it is mostly governed by $\eta^{(1)}$—the parameter defined in the incidence plane $[x_2, x_3]$. Whereas the magnitude of the dip line A_4 typically becomes small for dips exceeding 45°, the nonhyperbolic moveout on the strike line may remain significant even for subvertical reflectors. The character of the azimuthal variation of A_4 depends on reflector dip and is quite sensitive to the signs and relative magnitudes of $\eta^{(1)}$, $\eta^{(2)}$, and $\eta^{(3)}$. The analytic results and numerical modeling show that the azimuthal pattern of the quartic coefficient can contain multiple lobes, with one or two azimuths of vanishing A_4 between the dip and strike directions.

The strong influence of the anellipticity parameters on the azimuthally varying coefficient A_4 suggests that nonhyperbolic moveout recorded in wide-azimuth surveys can help to constrain the anisotropic velocity field. Since for typical orthorhombic models that describe naturally fractured reservoirs the parameters $\eta^{(1,2,3)}$ are closely related to the fracture density and infill, the results of azimuthal nonhyperbolic moveout analysis can also be used in reservoir characterization.

INTRODUCTION

Although most seismic processing algorithms are limited to analysis of hyperbolic moveout on moderate-length spreads, acquisition of long-offset data becomes more and more common. In particular, the technology of ocean-bottom cable is well suited for recording reflected waves for a wide range of offsets and source–receiver azimuths. The azimuthal dependence of nonhyperbolic reflection moveout at large offsets is strongly influenced by elastic anisotropy (Sayers and Ebrom, 1997; Al-Dajani and Tsvankin, 1998) and, therefore, can help in estimating the anisotropic parameters.

In velocity analysis of pure (unconverted) waves, nonhyperbolic moveout is conventionally described using the quartic moveout coefficient A_4. Tsvankin and Thomsen (1994) combined the coefficient A_4 with the NMO velocity V_{nmo} in a nonhyperbolic moveout equation that proved to be accurate for P-waves and converted PS-waves in horizontally layered anisotropic models (Tsvankin, 2001; Al-Dajani and Tsvankin, 1998). However, while the formalism for modeling NMO velocity in arbitrarily anisotropic, heterogeneous media has been developed by Grechka and Tsvankin (1998b, 2002) and Grechka, Tsvankin, and Cohen (1999), derivation of the quartic moveout coefficient proved to be much more involved because A_4 depends on reflection-point dispersal.

In our previous paper (Pech et al., 2003; hereafter referred to as Paper I), we presented a general equation for the coefficient A_4 of pure (unconverted) modes that takes into account reflection-point dispersal on irregular (but sufficiently smooth) interfaces and is valid for arbitrary anisotropy and heterogeneity. It should be emphasized that this result can be used to model long-spread moveout without time-consuming multioffset, multiazimuth ray tracing because all needed quantities can be computed during the tracing of the zero-offset ray. Note, however, that A_4 depends on fourth-order derivatives of traveltime, which implies that the smoothness of the model

Manuscript received by the Editor July 15, 2003; revised manuscript received November 11, 2003.
*Formerly Colorado School of Mines, Center for Wave Phenomena, Department of Geophysics Golden, Colorado 80401-1887; presently Instituto Politecnico Nacional, CIIDIR–Unidad Oaxaca, Calle Hornos 1003, Santa Cruz Xoxocotlan, Oaxaca, Mexico. E-mail: andrespech@yahoo.com.
‡Colorado School of Mines, Center for Wave Phenomena, Department of Geophysics, Golden, Colorado 80401-1887. E-mail: ilya@dix.mines.edu.

should be higher than that required in conventional second-order dynamic ray tracing.

For horizontally layered transversely isotropic (TI) models with a vertical (VTI) and horizontal (HTI) symmetry axis, the equation for A_4 from Paper I reduces to the known expressions given in Tsvankin (2001) and Al-Dajani and Tsvankin (1998). To evaluate the influence of anisotropy on the quartic moveout coefficient for models with reflection-point dispersal, in Paper I we study the behavior of A_4 in a dipping TI layer with a tilted symmetry axis. For weak anisotropy, the coefficient A_4 and the magnitude of nonhyperbolic moveout for P-waves in TI media are proportional to the anellipticity parameter η, defined as (Alkhalifah and Tsvankin, 1995)

$$\eta \equiv \frac{\epsilon - \delta}{1 + 2\delta}. \tag{1}$$

Paper I shows that the azimuthal variation of A_4 is highly sensitive to the tilt of the symmetry axis and reflector dip.

Here, we use the expression for the coefficient A_4 given in Paper I to analyze nonhyperbolic moveout from dipping reflectors for the more complicated azimuthally anisotropic models with orthorhombic symmetry often used to describe naturally fractured reservoirs (e.g., Bakulin et al., 2000). For the special case of a horizontal orthorhombic layer, our results are in good agreement with those of Al-Dajani et al. (1998). Valuable insight is provided by the weak-anisotropy approximation that expresses A_4 as a function of the three anellipticity parameters ($\eta^{(1)}$, $\eta^{(2)}$, and $\eta^{(3)}$) defined in the symmetry planes of the model. Numerical examples illustrate the complicated multilobe shape of the azimuthally varying coefficient A_4 and its dependence on the parameters $\eta^{(1,2,3)}$ and reflector dip.

NONHYPERBOLIC MOVEOUT AND THE QUARTIC MOVEOUT COEFFICIENT

A detailed analytic description of nonhyperbolic moveout in anisotropic media can be found in Tsvankin (2001). The nonhyperbolic portion of the moveout curve is governed by the quartic moveout coefficient A_4 defined by expanding the squared reflection traveltime t^2 in a Taylor series in the squared source–receiver offset X^2:

$$A_4 = \frac{1}{2}\frac{d}{d(X^2)}\left[\frac{d(t^2)}{d(X^2)}\right]\Bigg|_{X=0}. \tag{2}$$

Long-spread moveout of P-waves (and, for some models, PS-waves) in both isotropic and anisotropic media can be well approximated by the following equation suggested by Tsvankin and Thomsen (1994):

$$t^2 = t_0^2 + \frac{X^2}{V_{\text{nmo}}^2} + \frac{A_4 X^4}{1 + AX^2}, \tag{3}$$

where t_0 is the zero-offset time, V_{nmo} is the NMO velocity, and the denominator of the nonhyperbolic term is designed to make the equation convergent at infinitely large offsets. The coefficient A is expressed through V_{nmo}, A_4, and the horizontal group velocity V_{hor} as

$$A = \frac{A_4}{V_{\text{hor}}^{-2} - V_{\text{nmo}}^{-2}}. \tag{4}$$

The NMO velocity for anisotropic, heterogeneous media can be found from the Dix-type averaging equations developed by Grechka, Tsvankin, and Cohen (1999) and Grechka and Tsvankin (2002). An analytic expression for the quartic coefficient A_4 that has the same level of generality is introduced in Paper I. Since both V_{nmo} and A_4 can be computed by tracing only one (zero-offset) ray, equation (3) can serve as a computationally efficient replacement for full-scale anisotropic ray tracing in modeling and inversion algorithms.

Paper I shows that the quartic moveout coefficient A_4 is a function of the spatial derivatives of the one-way traveltime τ between the common midpoint $\mathbf{y}$ and point $\mathbf{x}$ on the reflector (Figure 1):

$$A_4(\mathbf{L}) = \frac{1}{16}\left[\frac{\partial^2\tau}{\partial y_k \partial y_l}\frac{\partial^2\tau}{\partial y_m \partial y_n} + \frac{\tau_0}{3}\frac{\partial^4\tau}{\partial y_k \partial y_l \partial y_m \partial y_n} - \tau_0 \frac{\partial^3\tau}{\partial y_k \partial y_l \partial x_i}\left(\frac{\partial^2\tau}{\partial x_i \partial x_j}\right)^{-1}\frac{\partial^3\tau}{\partial x_j \partial y_m \partial y_n}\right] L_k L_l L_m L_n. \tag{5}$$

Here, $\mathbf{L} = [\cos\alpha, \sin\alpha, 0]$ is a unit vector parallel to the CMP line with the azimuth α and τ_0 is the one-way zero-offset traveltime; summation over repeated indices from one to two is implied. All derivatives of τ are evaluated for the zero-offset reflection ray at the CMP location $\mathbf{y}$. Equation (5) is valid for arbitrarily anisotropic, heterogeneous media and irregular (but sufficiently smooth) reflectors, as long as reflection traveltime can be expanded in a Taylor series near the common midpoint.

Simplifying the spatial derivatives of τ in equation (5) under the assumption of weak anisotropy provides insight into the influence of the medium parameters on A_4 and nonhyperbolic moveout as a whole. Below, we obtain the weak-anisotropy approximation for A_4 in an orthorhombic layer and discuss its dependence on the anisotropic parameters and reflector dip.

BRIEF DESCRIPTION OF ORTHORHOMBIC MEDIA

Models with orthorhombic symmetry are often used to describe naturally fractured reservoirs that contain, for example, two orthogonal fracture systems or a single system of penny-shaped cracks embedded in a VTI matrix (e.g., Bakulin et al.,

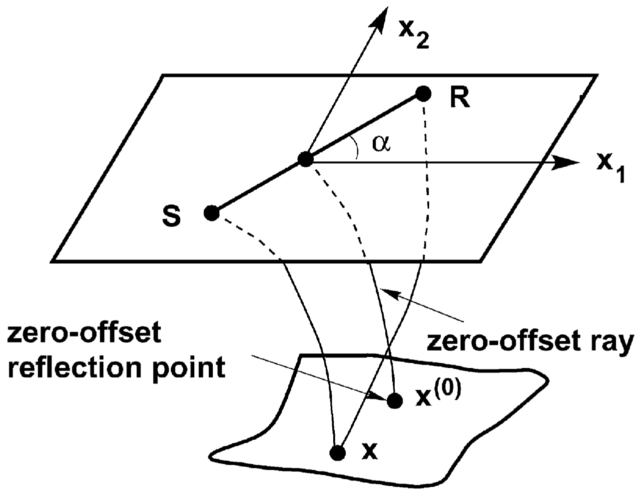

Figure 1. Reflection traveltimes from an irregular interface beneath an arbitrarily anisotropic, heterogeneous medium are recorded in a multiazimuth CMP gather. The quartic moveout coefficient A_4, which depends on reflection-point dispersal, varies with the azimuth α of the CMP line (after Paper I).

2000; Tsvankin, 2001). Orthorhombic media have three mutually orthogonal planes of mirror symmetry, one of which we assume to be horizontal.

Apart from the wavefront distortions near point shear-wave singularities (such as point A in Figure 2), velocities and traveltimes in the symmetry planes of orthorhombic media can be described by the corresponding VTI equations. That is one of the reasons why reflection moveout and other seismic signatures in orthorhombic media are particularly convenient to represent using the notation of Tsvankin (1997, 2001) based on the analogy with Thomsen's (1986) VTI parameters. Tsvankin's (1997, 2001) notation includes the anisotropic coefficients $\epsilon^{(1,2)}$, $\delta^{(1,2,3)}$, and $\gamma^{(1,2)}$ and the vertical velocities of the P-wave (V_{P0}) and the S-wave polarized in the x_1-direction (V_{S0}). The parameters $\epsilon^{(1)}$, $\delta^{(1)}$, and $\gamma^{(1)}$ are introduced in the vertical symmetry plane $[x_2, x_3]$ using the definitions of Thomsen's (1986) coefficients ϵ, δ, and γ for VTI media (Figure 2). Similarly, $\epsilon^{(2)}$, $\delta^{(2)}$, and $\gamma^{(2)}$ are defined in the $[x_1, x_3]$-plane, and $\delta^{(3)}$ is defined in the horizontal plane $[x_1, x_2]$.

An important role in the analysis of the quartic moveout coefficient below is played by the parameters $\eta^{(1)}$, $\eta^{(2)}$, and $\eta^{(3)}$, which quantify deviations from the elliptically anisotropic model in the symmetry planes (Grechka and Tsvankin, 1999):

$$\eta^{(1)} \equiv \frac{\epsilon^{(1)} - \delta^{(1)}}{1 + 2\delta^{(1)}} \approx \epsilon^{(1)} - \delta^{(1)}, \tag{6}$$

$$\eta^{(2)} \equiv \frac{\epsilon^{(2)} - \delta^{(2)}}{1 + 2\delta^{(2)}} \approx \epsilon^{(2)} - \delta^{(2)}, \tag{7}$$

$$\eta^{(3)} \equiv \frac{\epsilon^{(1)} - \epsilon^{(2)} - \delta^{(3)}\left(1 + 2\epsilon^{(2)}\right)}{\left(1 + 2\epsilon^{(2)}\right)\left(1 + 2\delta^{(3)}\right)} \approx \epsilon^{(1)} - \epsilon^{(2)} - \delta^{(3)}. \tag{8}$$

The approximate expressions for $\eta^{(1,2,3)}$ in equations (6)–(8) are obtained by linearizing the exact equations in the anisotropic parameters. In the definition of $\eta^{(3)}$, the axis x_1 plays the role of the symmetry axis of the equivalent TI medium.

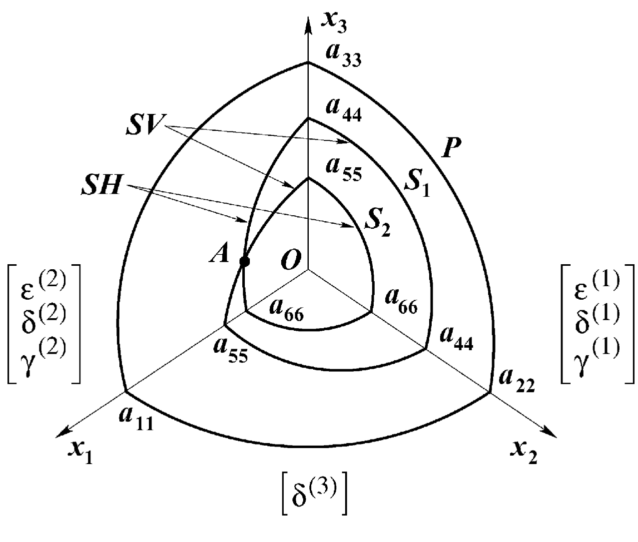

Figure 2. Sketch of body-wave phase-velocity surfaces in orthorhombic media (after Grechka, Theophanis, and Tsvankin, 1999). The fast shear wave represents an SH mode in the $[x_1, x_3]$-plane and an SV (in-plane polarized) mode in the $[x_2, x_3]$-plane. Point A marks a conical (point) singularity where the phase velocities of the two shear waves coincide with each other.

P-WAVE QUARTIC COEFFICIENT IN A DIPPING ORTHORHOMBIC LAYER

Our model consists of a homogeneous orthorhombic layer with a horizontal symmetry plane above a plane dipping reflector (Figure 3). The other two symmetry planes of the layer are vertical and coincide with the coordinate planes $[x_1, x_3]$ and $[x_2, x_3]$. For simplicity, we assume that the plane $[x_1, x_3]$ is also parallel to the dip plane of the reflector, which makes $[x_1, x_3]$ the only symmetry plane for the model as a whole. Therefore, as in isotropic or VTI media, the zero-offset reflected ray has to be confined to the dip plane (Figure 3), which would not be the case for arbitrary orientation of the vertical symmetry planes.

Weak-anisotropy approximation

The weak-anisotropy approximation for the P-wave quartic coefficient A_4 in this model is derived in Appendix A by linearizing the exact equation (5) in the anisotropic parameters:

$$A_4 = -\frac{1}{2t_{P0}^2 V_{P0}^4}\{\eta^{(2)}\cos^2\phi[2\cos 2\phi\,(1 + \cos 2\alpha\cos 2\phi) + \cos 4\phi - 1] + 4\eta^{(1)}\cos^2\phi\sin^2\alpha - 2\eta^{(3)}\sin^2\alpha\,(\cos 2\alpha + \cos 2\phi)\}, \tag{9}$$

where t_{P0} is the two-way zero-offset P-wave traveltime, ϕ is the reflector dip, α is the azimuth with respect to the dip plane $[x_1, x_3]$, and $\eta^{(1)}$, $\eta^{(2)}$, and $\eta^{(3)}$ are the anellipticity parameters defined in equations (6)–(8). Equation (9) shows that the azimuthal variation $A_4(\alpha)$ is controlled just by the parameters $\eta^{(1,2,3)}$ and dip ϕ. This result is not surprising because the parameters $\eta^{(1,2,3)}$, in combination with the NMO velocities from a horizontal reflector in the vertical symmetry planes, fully describe P-wave time-domain signatures for homogeneous orthorhombic media (Grechka and Tsvankin, 1999).

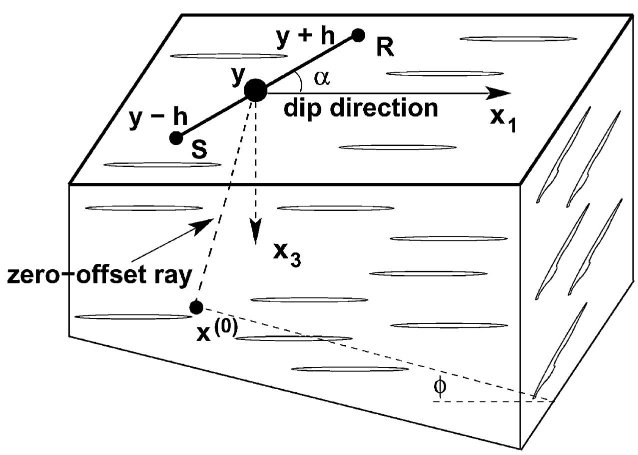

Figure 3. A reflected wave is recorded above a homogeneous orthorhombic layer with a dipping lower boundary. The vertical symmetry plane $[x_1, x_3]$ coincides with the dip plane of the reflector (the dip is denoted by ϕ).

Note that the quartic coefficient is symmetric not only with respect to the dip direction of the reflector (the dip plane $\alpha = 0^\circ$ is a symmetry plane for the whole model) but also with respect to the reflector strike. Indeed, since $A_4(\alpha) = A_4(-\alpha)$ and $A_4(\alpha) = A_4(\alpha \pm \pi)$, it follows that $A_4(\alpha) = A_4(\pi - \alpha)$, which means that the quartic coefficient is symmetric with respect to the strike direction $\alpha = \pm\pi/2$.

Figure 4 confirms that equation (9) is suitable for a qualitative description of the azimuthal signature of the quartic moveout coefficient for small and moderate values of the anisotropic parameters. Note that the magnitude of the η parameters in Figure 4 is quite substantial for fracture-induced orthorhombic media (Bakulin et al., 2000). Application of the quartic coefficient in velocity analysis, however, should not be based on the weak-anisotropy approximation, as is shown by Tsvankin and Thomsen (1994) for the simpler VTI model.

Special cases

If the reflector is horizontal ($\phi = 0^\circ$), equation (9) yields the linearized version of the exact solution for A_4 in a horizontal orthorhombic layer given by Al-Dajani et al. (1998):

$$A_4(\phi = 0^\circ) = -\frac{2}{t_{P0}^2 V_{P0}^4}\big(\eta^{(2)}\cos^2\alpha - \eta^{(3)}\cos^2\alpha\sin^2\alpha + \eta^{(1)}\sin^2\alpha\big). \qquad (10)$$

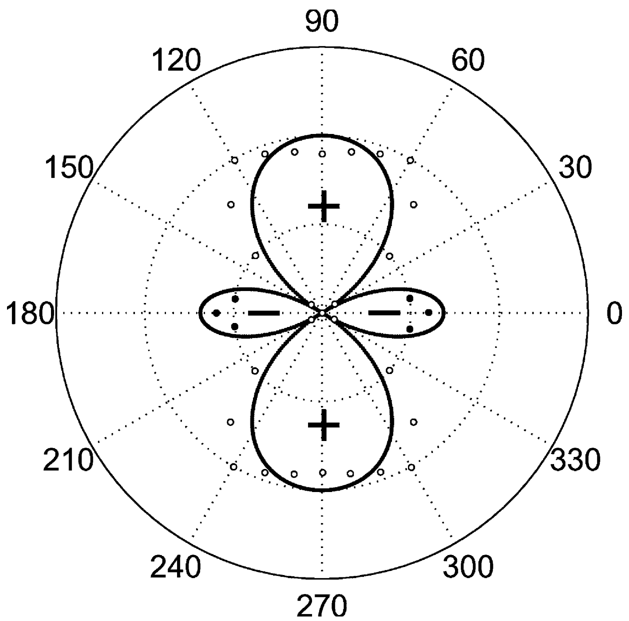

Figure 4. Accuracy of the weak-anisotropy approximation for the coefficient A_4 in an orthorhombic layer with the lower boundary dipping at $\phi = 15^\circ$. The circles mark the magnitude of A_4 obtained for each azimuth (the numbers on the perimeter; zero azimuth corresponds to the dip plane) by fitting a quartic polynomial to the ray-traced $t^2(x^2)$-curve on the spread length $X_{\max} = 1.5$ km; the reflector depth beneath the CMP is 1 km. The white circles mark positive values of A_4; the black circles mark negative A_4. The solid line is the weak-anisotropy approximation (9); the pluses and minuses indicate the signs of A_4 in the corresponding lobes. Both the ray-tracing and weak-anisotropy results are normalized by their respective maximum values of $|A_4|$. The anellipticity parameters are $\eta^{(1)} = -0.2$, $\eta^{(2)} = 0.2$, and $\eta^{(3)} = 0.2$.

Although equation (10) is an approximation valid for small values of the anisotropic coefficients, our analysis shows that it accurately reproduces the azimuthal variation of the quartic coefficient. For a horizontal layer, A_4 in both symmetry-plane directions ($\alpha = 0^\circ$ and 90°) depends just on the corresponding in-plane η-parameter ($\eta^{(2)}$ in the $[x_1, x_3]$-plane and $\eta^{(1)}$ in the $[x_2, x_3]$-plane). The coefficient $\eta^{(3)}$ contributes only to the crossterm that reaches its maximum at the azimuth $\alpha = 45^\circ$.

Another special case is that of a dipping VTI layer since TI models can be treated as a subset of the more general orthorhombic media. The quartic coefficient in VTI media, which is derived and analyzed in Paper I, can be found from equation (9) by setting $\eta^{(1)} = \eta^{(2)} = \eta$ and $\eta^{(3)} = 0$ (Tsvankin, 1997):

$$A_4^{\text{VTI}} = -\frac{2\eta}{t_{P0}^2 V_{P0}^4}\cos^4\phi\,(1 - 4\sin^2\phi\cos^2\alpha). \qquad (11)$$

The dip-line ($\alpha = 0^\circ$) and strike-line ($\alpha = 90^\circ$) coefficients A_4 for VTI media, which we will need below for comparison with the expressions for orthorhombic media, are

$$A_{4,\text{dip}}^{\text{VTI}} = -\frac{2\eta}{t_{P0}^2 V_{P0}^4}\cos^4\phi\,(1 - 4\sin^2\phi) \qquad (12)$$

and

$$A_{4,\text{strike}}^{\text{VTI}} = -\frac{2\eta}{t_{P0}^2 V_{P0}^4}\cos^4\phi. \qquad (13)$$

Dip-line and strike-line expressions

As discussed above, the azimuthally varying quartic coefficient in our model is symmetric with respect to the dip and strike directions of the reflector. On the dip line ($\alpha = 0^\circ$), the coefficient A_4 from equation (9) takes the form

$$A_{4,\text{dip}} = -\frac{2\eta^{(2)}}{t_{P0}^2 V_{P0}^4}\cos^4\phi\,(1 - 4\sin^2\phi). \qquad (14)$$

Equation (14) becomes identical to the corresponding VTI equation (12) if the parameter $\eta^{(2)}$ is replaced with η. Indeed, reflected rays (and their phase-velocity vectors) on the dip line are confined to the symmetry plane $[x_1, x_3]$ where the kinematics of wave propagation are the same as those in the VTI model with the vertical velocities V_{P0} and V_{S0} and the anisotropic parameters $\epsilon = \epsilon^{(2)}$, $\delta = \delta^{(2)}$ (so $\eta = \eta^{(2)}$), and $\gamma = \gamma^{(2)}$ (Tsvankin, 1997, 2001).

The combined influence of the factors $\cos^4\phi$ and $(1 - 4\sin^2\phi)$ in equation (14) leads to a rapid decrease of the magnitude of the dip-line quartic coefficient with ϕ at mild dips, and $A_{4,\text{dip}} = 0$ for $\phi = 30^\circ$. If $\eta^{(2)} > 0$, the coefficient $A_{4,\text{dip}}$ is negative for $\phi < 30^\circ$ and becomes positive for $\phi > 30^\circ$, as discussed in Paper I for VTI media (also, see the related numerical results in Tsvankin, 1995, 2001). Unless the magnitude of $\eta^{(2)}$ is uncommonly large, the factor $\cos^4\phi$ makes $A_{4,\text{dip}}$ almost negligible for dips exceeding 45°.

Substitution of $\alpha = 90^\circ$ into equation (9) yields the strike-line quartic coefficient:

$$A_{4,\text{strike}} = -\frac{2}{t_{P0}^2 V_{P0}^4}\big(\eta^{(1)}\cos^2\phi - \eta^{(2)}\cos^2\phi\sin^2\phi + \eta^{(3)}\sin^2\phi\big). \qquad (15)$$

It is interesting that the functional dependence of $A_{4,\mathrm{strike}}$ on the dip ϕ is similar to that of the quartic coefficient in a horizontal layer on the azimuth α [equation (10)]. In contrast to the coefficient $A_{4,\mathrm{dip}}$, $A_{4,\mathrm{strike}}$ depends on all three parameters $\eta^{(1,2,3)}$ because reflected rays recorded on the strike line x_2 deviate from the vertical symmetry plane $[x_2, x_3]$. For the same reason, $A_{4,\mathrm{strike}}$ differs from the strike-line coefficient in VTI media [equation (13)] with $\eta = \eta^{(1)}$ (the parameter $\eta^{(1)}$ is defined in the $[x_2, x_3]$-plane). However, equation (15) indicates that $\eta^{(1)}$ does control the quartic coefficient for mild reflector dips ϕ.

Unlike the quartic coefficient on the dip line, $A_{4,\mathrm{strike}}$ does not always decrease by absolute value with reflector dip. The function $A_{4,\mathrm{strike}}(\phi)$ is governed by the relative magnitudes of the three anellipticity coefficients and becomes largely dependent on $\eta^{(3)}$ for steep dips. If the interface is vertical ($\phi = 90^\circ$), reflected rays travel in the horizontal symmetry plane, and the strike-line quartic coefficient reduces to

$$A_{4,\mathrm{strike}}(\phi = 90^\circ) = -\frac{2\eta^{(3)}}{t_{P0}^2 V_{P0}^4}. \qquad (16)$$

Equation (16) coincides with the weak-anisotropy approximation for A_4 in a horizontal VTI layer with $\eta = \eta^{(3)}$. Therefore, if $|\eta^{(3)}| > |\eta^{(1)}|$, the magnitude of $A_{4,\mathrm{strike}}$ for a vertical reflector is higher than that for a horizontal reflector.

Azimuthal signature

The azimuthal variation of the quartic coefficient from equation (9) strongly depends on reflector dip as well as the magnitudes and signs of the anellipticity parameters $\eta^{(1,2,3)}$. For mild dips, $A_4(\alpha)$ is largely controlled by the parameters $\eta^{(1)}$ (near the $[x_2, x_3]$-plane) and $\eta^{(2)}$ (near the $[x_1, x_3]$-plane), with the influence of $\eta^{(3)}$ typically being relatively weak [see equation (10)]. As illustrated by Figure 5, if both $\eta^{(1)}$ and $\eta^{(2)}$ are positive and much greater by absolute value than $\eta^{(3)}$, A_4 typically stays negative for dips smaller than 30°; the same result is obtained in Paper I for a dipping VTI layer [see equation (11)]. Also, as in VTI media, for a dip of 30° A_4 goes to zero only in the single (dip) direction (Figure 6), although it remains small for $|\alpha| < 30^\circ$.

For the η parameters used in Figures 5 and 6 and dips between 30° and 90°, equation (9) yields two azimuths $\pm\alpha$ for which $A_4 = 0$. If the dip $\phi = 45^\circ$ (Figure 7), the quartic coefficient is positive near the dip plane, vanishes at $\alpha \approx \pm 60^\circ$, and becomes negative close to the strike direction. Although typically we expect the quartic coefficient for dips $\phi > 45^\circ$ to be larger in the strike direction than in the dip plane, for the model in Figure 7 the strike line A_4 is small because the terms involving $\eta^{(1)}$ and $\eta^{(2)}$ in equation (15) almost cancel each other.

The azimuthal variation of the quartic coefficient has a different character if $\eta^{(1)}$ and $\eta^{(2)}$ have opposite signs. In this case, for mild dips A_4 changes sign between the dip and strike directions [see equations (14) and (15)], with the azimuthal direction of vanishing A_4 dependent on dip and the relative magnitudes of $\eta^{(1)}$ and $\eta^{(2)}$ (Figure 8). Since the quartic coefficient decreases with the dip ϕ more rapidly in the dip plane than in the strike direction, the direction where $A_4 = 0$ rotates toward the dip plane as ϕ increases. For a dip of 15° (Figure 8), A_4 goes to zero at the angle $\alpha \approx \pm 35^\circ$ from the dip plane. When the dip reaches 30° (Figure 9), the quartic coefficient goes to zero in the dip direction and the azimuthal variation of A_4 is similar to that in Figure 6. However, the sign of A_4 away from the dip plane in Figure 9 is positive because $\eta^{(1)} < 0$. Finally, for dips larger than 30°, the quartic coefficient is positive for all azimuths (Figure 10).

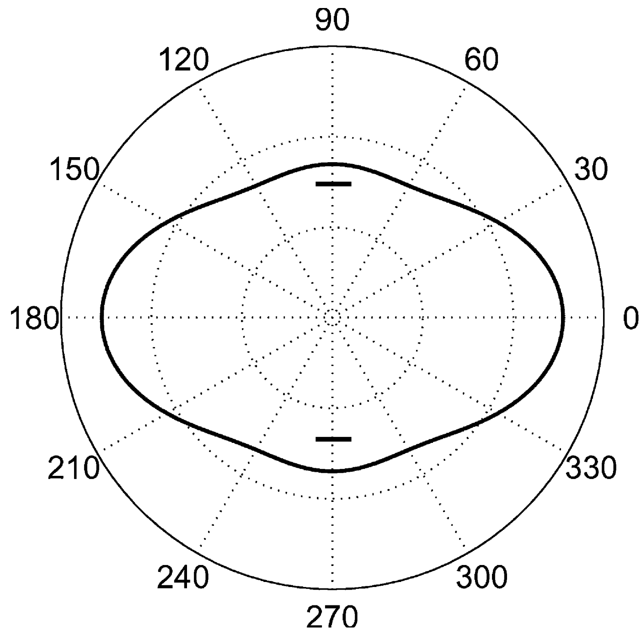

Figure 5. Magnitude of the azimuthally varying quartic moveout coefficient A_4 for a dipping orthorhombic layer computed from equation (9). The dip plane of the reflector is at zero azimuth (the azimuth is marked on the perimeter). The anellipticity parameters are $\eta^{(1)} = 0.05$, $\eta^{(2)} = 0.1$, and $\eta^{(3)} = 0.03$; the reflector dip $\phi = 15^\circ$. The other parameters (t_{P0} and V_{P0}) change only the scale of the plot (intentionally undefined here). For this model, $A_4 < 0$ for all azimuthal directions.

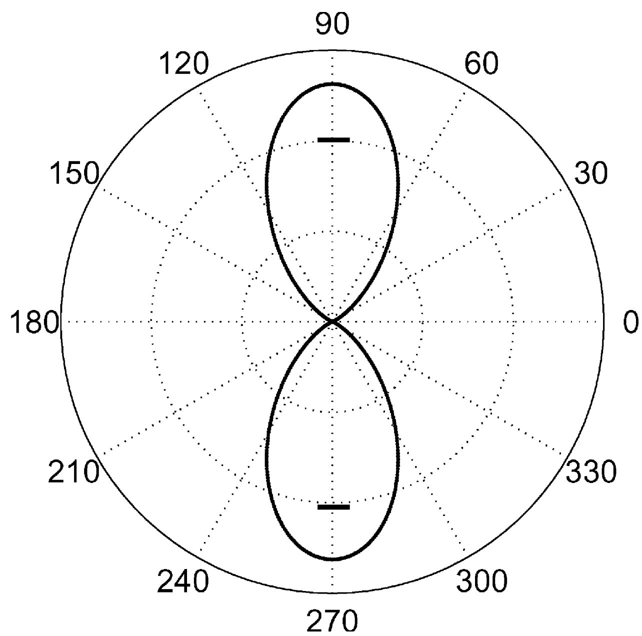

Figure 6. Same as Figure 5, but the reflector dip is 30°. The minus signs inside the lobes indicate negative values of A_4.

To analyze the influence of the parameter $\eta^{(3)}$ on the quartic coefficient, in the next two examples (Figures 11 and 12) we set $\eta^{(1)}$ and $\eta^{(2)}$ to zero. Clearly, the term involving $\eta^{(3)}$ creates a rather complicated azimuthal signature of A_4. Since the dip-line coefficient $A_{4,\mathrm{dip}}$ [equation (14)] is proportional to $\eta^{(2)}$, it vanishes for all dips when $\eta^{(2)} = 0$. In addition, A_4 goes to zero for another azimuth near the strike direction, even for a dip of just 15° (Figure 11). The azimuthal variation of A_4 for $\phi = 30°$ has a similar general character but with completely different relative magnitudes of the lobes (Figure 12).

For nonzero values of $\eta^{(1)}$ and $\eta^{(2)}$, the contribution of the term proportional to $\eta^{(3)}$ generally increases with reflector dip (Figures 13–15). While the dip-line coefficient A_4 depends just on $\eta^{(2)}$, $A_{4,\mathrm{strike}}$ is significantly influenced by $\eta^{(3)}$, in particular for dips exceeding 30°. If $\eta^{(3)}$ is larger by absolute value than $\eta^{(1)}$ and $\eta^{(2)}$, the quartic coefficient typically goes to zero in at least one off-symmetry direction for a wide range of dips. For example, if $\phi = 30°$, the influence of $\eta^{(3)}$ produces an additional direction of vanishing A_4 near the reflector strike, and

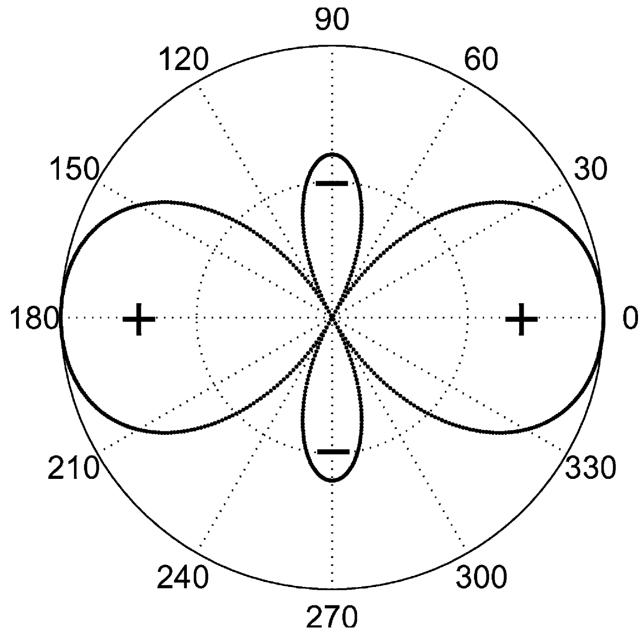

Figure 7. Same as Figure 5, but the reflector dip is 45°.

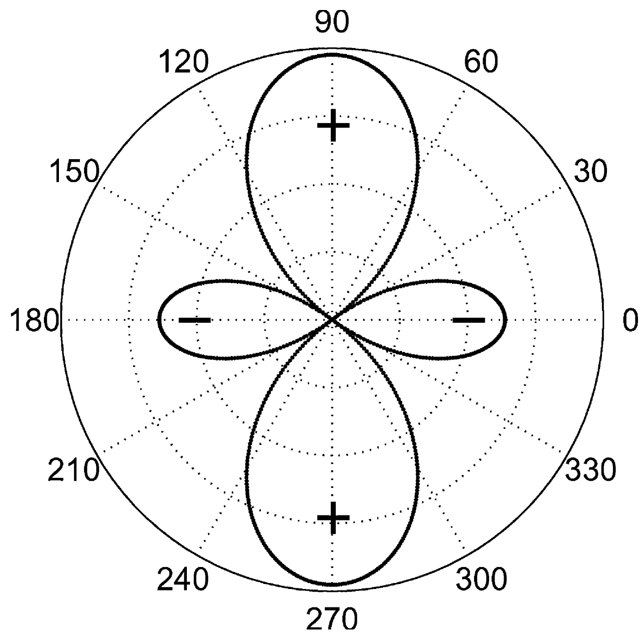

Figure 8. Magnitude of the quartic moveout coefficient A_4 for an orthorhombic layer computed from equation (9). The anellipticity parameters are $\eta^{(1)} = -0.1$, $\eta^{(2)} = 0.1$, and $\eta^{(3)} = 0.03$; the reflector dip $\phi = 15°$.

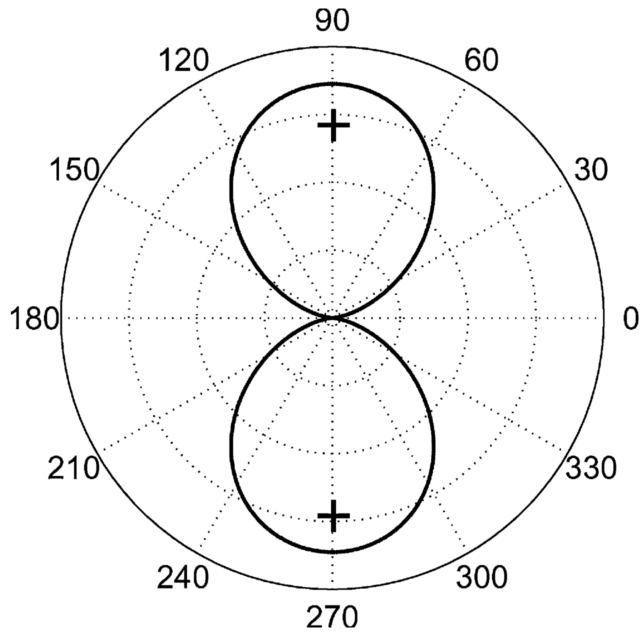

Figure 9. Same as Figure 8, but the reflector dip is 30°.

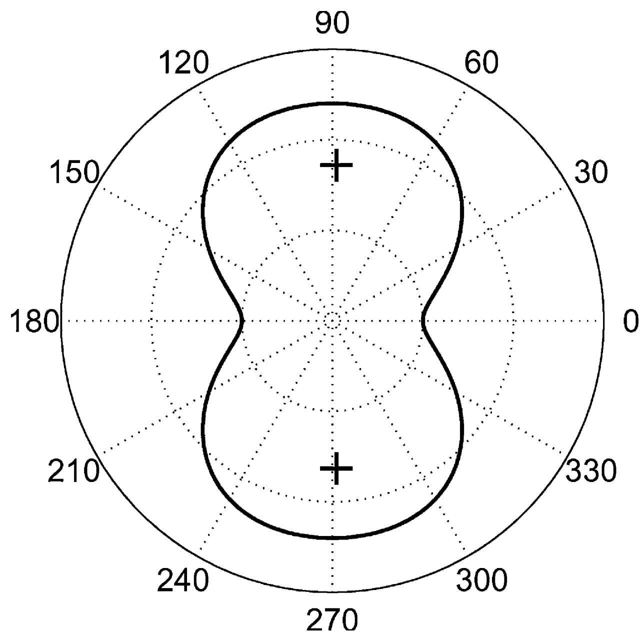

Figure 10. Same as Figure 8, but the reflector dip is 45°.

the azimuthal variation of the quartic coefficient is described by six lobes[1] with alternating signs from one lobe to the next (Figure 14).

[1]Only three lobes are independent because $A_4(\alpha) = A_4(\alpha \pm \pi)$.

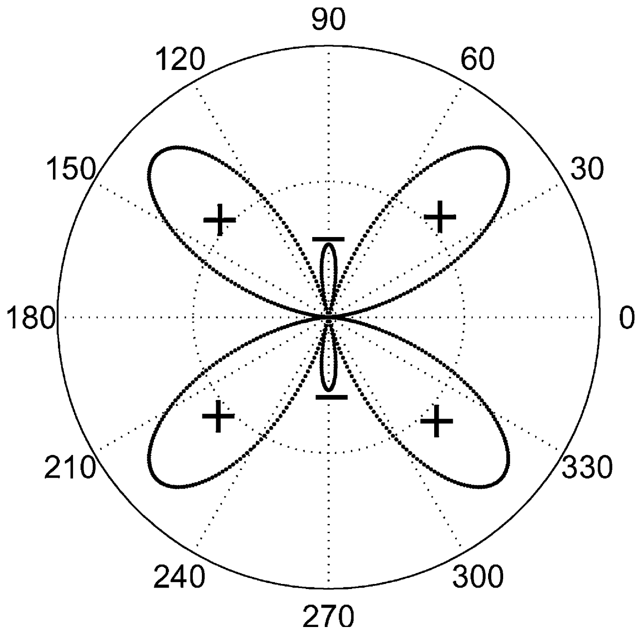

Figure 11. Magnitude of the quartic moveout coefficient A_4 for an orthorhombic layer computed from equation (9). The anellipticity parameters are $\eta^{(1)} = \eta^{(2)} = 0$ and $\eta^{(3)} = 0.1$; the reflector dip $\phi = 15^\circ$.

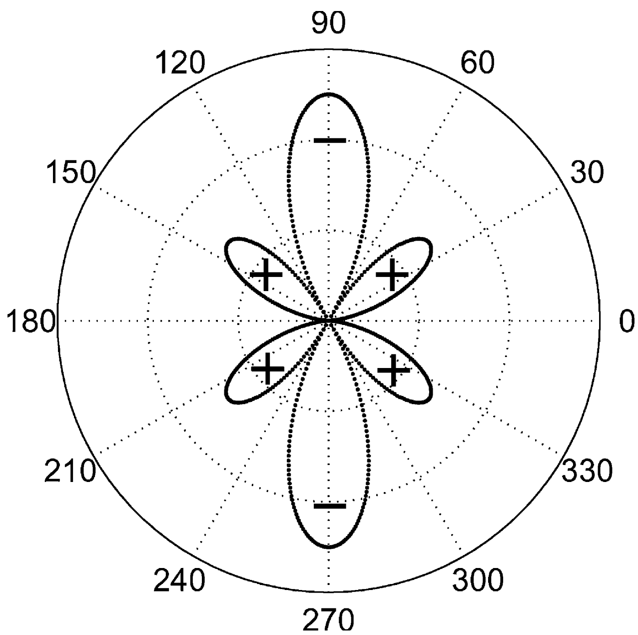

Figure 12. Same as Figure 11, but the reflector dip is 30°.

DISCUSSION AND CONCLUSIONS

The general expression for the quartic moveout coefficient A_4 derived by Pech et al. (2003; Paper I) was used here to study P-wave nonhyperbolic moveout in a dipping orthorhombic layer. Similar to the NMO ellipse, the coefficient A_4 can be computed by tracing a single (zero-offset) ray and then used in the nonhyperbolic moveout equation of Tsvankin and

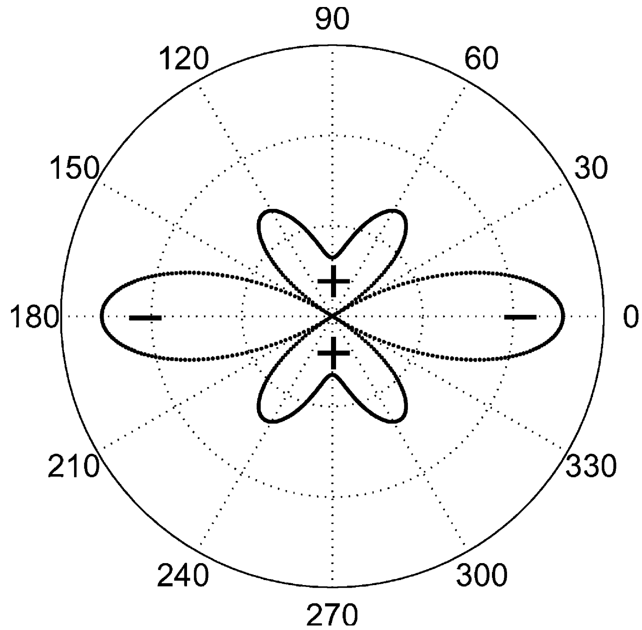

Figure 13. Magnitude of the quartic moveout coefficient A_4 for an orthorhombic layer computed from equation (9). The anellipticity parameters are $\eta^{(1)} = -0.025$, $\eta^{(2)} = 0.1$, and $\eta^{(3)} = 0.2$; the reflector dip $\phi = 15^\circ$.

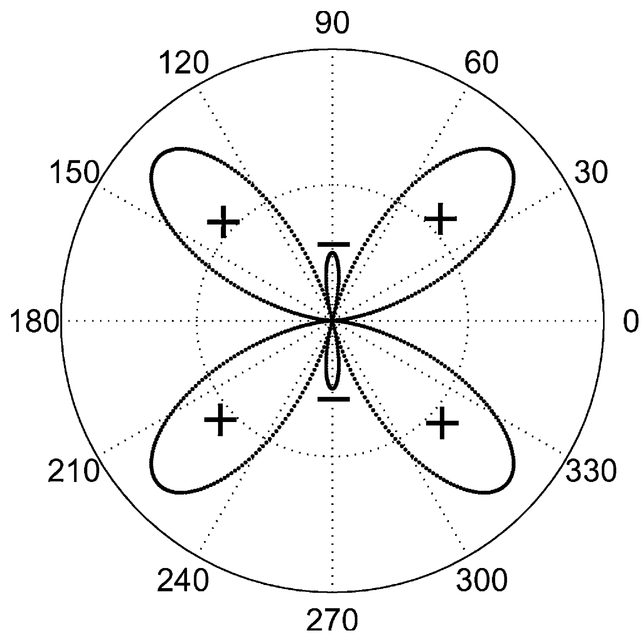

Figure 14. Same as Figure 13, but the reflector dip is 30°.

Thomsen (1994) to model reflection traveltimes without time-consuming ray tracing for each source–receiver pair. Note that the model has to be sufficiently smooth to allow for stable evaluation of the fourth-order spatial traveltime derivatives needed to obtain A_4.

The main emphasis of this paper, however, is on analysis of the azimuthal variation of the P-wave quartic moveout coefficient. The model consisted of a homogeneous orthorhombic layer with a horizontal symmetry plane and a dipping lower boundary (reflector). It was assumed that the dip plane of the reflector coincides with a vertical symmetry plane of the layer and, therefore, represents a symmetry plane for the whole model. Another symmetry direction for reflection moveout in this model is that of reflector strike, so the azimuthal signature of the quartic coefficient A_4 is repeated in each quadrant.

The weak-anisotropy approximation for A_4 linearized in Tsvankin's (1997) anisotropic parameters shows that the azimuthal dependence of the quartic coefficient is controlled by reflector dip and three anellipticity parameters $\eta^{(1,2,3)}$. It should be mentioned that the η-parameters, in combination with the two symmetry-direction NMO velocities, are responsible for all P-wave time-processing steps in homogeneous orthorhombic media, including NMO correction, DMO removal, and time migration.

The dip-line quartic coefficient $A_{4,\text{dip}}$ is described by the same equation as in VTI media and depends on a single (in-plane) anellipticity parameter $-\,\eta^{(2)}$. The coefficient $A_{4,\text{dip}}$ vanishes for the dip $\phi = 30^\circ$ and a vertical reflector (dip $\phi = 90^\circ$); the sign of $A_{4,\text{dip}}$ for $\phi < 30^\circ$ is opposite to that of $\eta^{(2)}$. Unless the magnitude of $\eta^{(2)}$ is uncommonly large, $A_{4,\text{dip}}$ becomes almost negligible for $\phi > 45^\circ$.

The analytic expression for the strike-line coefficient $A_{4,\text{strike}}$ contains all three η parameters, but for mild dips it is largely governed by $\eta^{(1)}$. Hence, if $\eta^{(1)}$ and $\eta^{(2)}$ have opposite signs, A_4 for mildly dipping reflectors changes sign between the dip and strike directions. The influence of $\eta^{(3)}$ generally increases with dip and may create a rather complicated azimuthal signature of the quartic coefficient, sometimes with two azimuths of vanishing A_4 in each quadrant. In contrast to the dip-line quartic coefficient, $A_{4,\text{strike}}$ does not necessarily decrease by absolute value with dip.

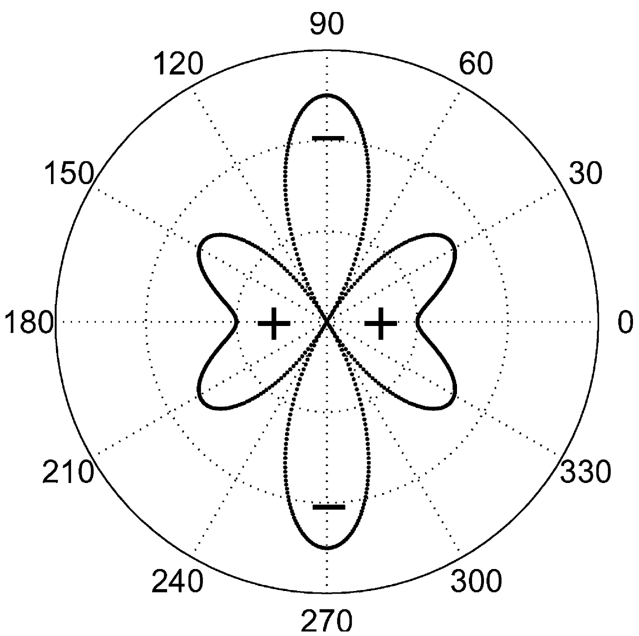

Figure 15. Same as Figure 13, but the reflector dip is 45°.

The high variability of the azimuthal signature of the quartic coefficient and its sensitivity to the time-processing parameters $\eta^{(1,2,3)}$ can be exploited in the inversion of P-wave data for orthorhombic media. Despite the known instability in estimating the quartic moveout coefficient (Grechka and Tsvankin, 1998a), we expect that wide-azimuth long-offset reflection data of sufficient quality may be used to determine the sign of A_4 and the azimuthal directions of its minimum values. This information can help in constraining the parameters $\eta^{(1,2,3)}$, which are not only needed in velocity analysis but can also be used in fracture characterization. For example, if the effective orthorhombic anisotropy is caused by two orthogonal systems of penny-shaped cracks embedded in isotropic host rock, all three η coefficients vanish for dry (gas-filled) cracks and are positive for cracks filled with fluid (Bakulin et al., 2000).

The exact equation for the quartic moveout coefficient from Paper I can be applied to model nonhyperbolic moveout in more complicated layered orthorhombic media. This work can provide useful insight into the behavior of A_4 in layered media because, for mild dips and moderate azimuthal anisotropy, the effective quartic coefficient at the surface can be computed from the interval values of A_4 for the same azimuth using the VTI averaging equations (Al-Dajani and Tsvankin, 1998; Al-Dajani et al., 1998).

ACKNOWLEDGMENTS

We are grateful to members of the A(nisotropy)-Team of the Center for Wave Phenomena (CWP), Colorado School of Mines, for useful discussions. We would like to thank the associate editor (Vladimir Grechka) and reviewers (Peter Bakker and Hongbo Zhou) of *Geophysics* for their comments and suggestions which helped to improve the manuscript. The support for this work was provided by the Consortium Project on Seismic Inverse Methods for Complex Structures at CWP and by the Chemical Sciences, Geosciences and Biosciences Division, Office of Basic Energy Sciences, U.S. Department of Energy.

APPENDIX A

WEAK-ANISOTROPY APPROXIMATION FOR THE QUARTIC MOVEOUT COEFFICIENT IN ORTHORHOMBIC MEDIA

Here we apply the approach discussed in Paper I to obtain a linearized approximation for the P-wave quartic coefficient A_4 in a homogeneous orthorhombic layer above a plane dipping reflector (Figure 3). It is assumed that the dip plane of the reflector coincides with the $[x_1, x_3]$ symmetry plane of the overburden; the other symmetry planes are $[x_1, x_2]$ and $[x_2, x_3]$.

The one-way traveltime between the CMP $\mathbf{y}$ and the plane reflector $z(x_1, x_2)$ is

$$\tau = \frac{\sqrt{(x_1 - y_1)^2 + (x_2 - y_2)^2 + z^2(x_1, x_2)}}{V_G}, \qquad \text{(A-1)}$$

where V_G is the group velocity. The orientation of the ray that connects the CMP with the reflector can be characterized by the polar angle a and the azimuthal angle b:

$$\sin a \equiv \frac{\sqrt{(y_1 - x_1)^2 + (y_2 - x_2)^2}}{\sqrt{(y_1 - x_1)^2 + (y_2 - x_2)^2 + z^2}}, \quad \text{(A-2)}$$

$$\cos a \equiv \frac{z}{\sqrt{(y_1 - x_1)^2 + (y_2 - x_2)^2 + z^2}}, \quad \text{(A-3)}$$

$$\sin b \equiv \frac{(y_2 - x_2)}{\sqrt{(y_1 - x_1)^2 + (y_2 - x_2)^2}}, \quad \text{(A-4)}$$

$$\cos b \equiv \frac{(y_1 - x_1)}{\sqrt{(y_1 - x_1)^2 + (y_2 - x_2)^2}}. \quad \text{(A-5)}$$

The P-wave group velocity V_G linearized in the anisotropic parameters can be determined from the weak-anisotropy approximation for the phase velocity given in Tsvankin (1997, 2001):

$$V_G = V_{P0}\big\{1 + \big(\epsilon^{(2)} - \delta^{(2)}\big)(\sin a \cos b)^4 + \delta^{(1)}(\sin a \sin b)^2 + \big(\epsilon^{(1)} - \delta^{(1)}\big)(\sin a \sin b)^4 + \cos^2 b\big[\delta^{(2)} \sin^2 a - \big(\delta^{(1)} + \delta^{(2)} - \delta^{(3)} - 2\epsilon^{(2)}\big) \sin^4 a \sin^2 b\big]\big\}; \quad \text{(A-6)}$$

the angles a and b are defined in equations (A-2)–(A-5).

Next, equation (A-1) with the velocity V_G from equation (A-6) is substituted into the general equation (5) to evaluate the spatial derivatives of the traveltime, which yields the quartic coefficient A_4 as a function of the coordinates of the CMP and the zero-offset reflection point. Since the zero-offset ray is confined to the dip plane $[x_1, x_3]$ where all kinematic signatures are described by the corresponding VTI equations, we can relate the CMP coordinates y_1 and y_2 to the horizontal coordinates $x_1^{(0)}$ and $x_2^{(0)}$ of the zero-offset reflection point by adapting the results of Paper I. Setting to zero the tilt ν of the symmetry axis in equations (B-11) and (B-12) from Paper I and replacing ϵ with $\epsilon^{(2)}$ and η with $\eta^{(2)}$ yields

$$y_1 = 2z^{(0)} \tan\phi\big[0.5 + \epsilon^{(2)} - \big(\epsilon^{(2)} - \delta^{(2)}\big)\cos 2\phi\big] + x_1^{(0)}, \quad \text{(A-7)}$$

$$y_2 = x_2^{(0)}; \quad \text{(A-8)}$$

$z^{(0)}$ is the depth of the zero-offset reflection point.

Using equations (A-7) and (A-8) and applying further linearization in the anisotropic parameters with the help of Mathematica symbolic software, we obtain the following approximation for the P-wave quartic moveout coefficient in orthorhombic media:

$$A_4 = -\frac{1}{2t_{P0}^2 V_{P0}^4}\big\{\eta^{(2)} \cos^2\phi\,[2\cos 2\phi(1 + \cos 2\alpha \cos 2\phi) + \cos 4\phi - 1] + 4\eta^{(1)} \cos^2\phi \sin^2\alpha - 2\eta^{(3)} \sin^2\alpha\,(\cos 2\alpha + \cos 2\phi)\big\}, \quad \text{(A-9)}$$

where t_{P0} is the two-way zero-offset traveltime and $\eta^{(1,2,3)}$ are the linearized versions of the anellipticity parameters defined in equations (6)–(8).

REFERENCES

Al-Dajani, A., and Tsvankin, I., 1998, Nonhyperbolic reflection moveout for horizontal transverse isotropy: Geophysics, **63**, 1738–1753.

Al-Dajani, A., Tsvankin, I., and Toksöz, M. N., 1998, Nonhyperbolic reflection moveout for azimuthally anisotropic media: 68th Annual International Meeting, Society of Exploration Geophysicists, Expanded Abstracts, 1479–1482.

Alkhalifah, T., and Tsvankin, I., 1995, Velocity analysis for transversely isotropic media: Geophysics, **60**, 1550–1566.

Bakulin, A., Grechka, V., and Tsvankin, I., 2000, Estimation of fracture parameters from reflection seismic data—Part II: Fractured models with orthorhombic symmetry: Geophysics, **65**, 1803–1817.

Grechka, V., and Tsvankin, I., 1998a, Feasibility of nonhyperbolic moveout inversion in transversely isotropic media: Geophysics, **63**, 957–969.

——— 1998b, 3-D description of normal moveout in anisotropic inhomogeneous media: Geophysics, **63**, 1079–1092.

——— 1999, 3-D moveout velocity analysis and parameter estimation for orthorhombic media: Geophysics, **64**, 820–837.

——— 2002, NMO-velocity surfaces and Dix-type formulas in heterogeneous anisotropic media: Geophysics, **67**, 939–951.

Grechka, V., Theophanis, S., and Tsvankin, I., 1999, Joint inversion of P- and PS-waves in orthorhombic media: Theory and a physical-modeling study: Geophysics, **64**, 146–161.

Grechka, V., Tsvankin, I., and Cohen, J.K., 1999, Generalized Dix equation and analytic treatment of normal-moveout velocity for anisotropic media: Geophysical Prospecting, **47**, 117–148.

Pech, A., Tsvankin, I., and Grechka, V., 2003, Quartic moveout coefficient: 3D description and application to tilted TI media: Geophysics, **68**, 1600–1610.

Sayers, C. M., and Ebrom, D. A., 1997, Seismic traveltime analysis for azimuthally anisotropic media: Theory and experiment: Geophysics, **36**, 1570–1582.

Thomsen, L., 1986, Weak elastic anisotropy: Geophysics, **51**, 1954–1966.

Tsvankin, I., 1995, Normal moveout from dipping reflectors in anisotropic media: Geophysics, **60**, 268–284.

——— 1997, Anisotropic parameters and P-wave velocity for orthorhombic media: Geophysics, **62**, 1292–1309.

——— 2001, Seismic signatures and analysis of reflection data in anisotropic media: Elsevier Science Publishing Company, Inc.

Tsvankin, I., and Thomsen, L., 1994, Nonhyperbolic reflection moveout in anisotropic media: Geophysics, **59**, 1290–1304.